INORGANIC
CHEMISTRY
FRONTIERS

RESEARCH ARTICLE

Thioether-terminated nickel(II) coordination clusters with {Ni6} horseshoe- and {Ni8} rollercoaster-shaped cores†

Sebastian Schmitz,[a] Jan van Leusen,[a] Arkady Ellern,[b] Paul Kögerler*[a,c] and Kirill Yu. Monakhov*[a]

We report two polynuclear nickel(II) compounds whose supramolecular structures are controlled by small inorganic templating anions and π-conjugated Schiff-base ligands (L·SMe^{3-} and HL·SMe^{2-}) with peripheral, structurally exposed methylthioether groups. The central component of the compound [Ni$_6$(L·SMe)$_3$(CO$_3$)(MeOH)$_6$(THF)$_2$]Cl·2MeOH (**1**, monoclinic space group $P2/c$) displays a horseshoe-shaped {Ni$_6$} core templated by μ$_6$-CO$_3^{2-}$ moiety due to the fixation of atmospheric carbon dioxide. According to thermogravimetric analysis, compound **1** retains the structural integrity of its carbonate-bonded metal core [Ni$_6$(L·SMe)$_3$(CO$_3$)]$^+$ up to *ca.* 390 °C. In the crystal lattice, compound **1** features an one-dimensional hydrogen-bonded chain structure [{CO$_3$ ⊂ Ni$_6$}···Cl···{CO$_3$ ⊂ Ni$_6$}]$_\infty$. The structure of the compound [Ni$_8$(HL·SMe)$_2$(L·SMe)$_2$(OH)$_4$(MeCN)$_4$(H$_2$O)$_4$](NO$_3$)$_2$·11MeCN·2PhCN (**2**, triclinic space group $P\bar{1}$) consists of a dicationic crown-like {Ni$_8$} metallamacrocycle hosting two NO$_3^-$ anions in the upper and lower cavities. The {Ni$_6$} complex is characterised by antiferromagnetic exchange interactions, whereas {Ni$_8$} reveals predominantly ferromagnetic exchange coupling between the spin-1 Ni(II) centres. The presence of terminal thioether anchoring groups at the periphery of complex **1**, coupled with high thermal stability and solubility in several common organic solvents, renders this compound an interesting candidate for molecular surface-deposition from solution using electrospray ionisation mass spectrometry approach and, possibly, for supported-transition metal complex heterogeneous catalysis.

Introduction

Fabrication of nanomaterials[1] with well-defined morphology and properties derived from the contact of individual coordination complexes and clusters of magnetic, electrochemical, and catalytic interest with a metallic substrate (electrode) attracts great attention in modern surface chemistry[2] and physics[3] and is motivated by the continual search for multi-functional, compact, and biocompatible structures for renewable and sustainable energy. The peripheral functionalisation of stimuli-responsive metalorganic compounds with the electron-rich "anchoring" groups[4] such as *e.g.* cyclic or acyclic thioether (–S–), 1,2-dithiolane (–S–S–) or thiol (–SH) constitutes one out of multiple chemical strategies[5] to anchor molecules to macroscopic solid-state electrodes[6] (*e.g.*, gold). The ligand environment of the metal centres as well as the structural, thermal and redox stability, solubility (for solution-driven molecular deposition), and volatility/sublimability (for deposition from the solid phase) of molecules are the key features in multilateral surface-oriented investigation toward hybrid catalytic systems and electronic devices.

The structural, spectroscopic, electrochemical, and catalytic properties of diamagnetic and paramagnetic S-terminated transition metal complexes and clusters were extensively studied during previous years: (i) electrochemical, electrocatalytic, and/or *in situ* infrared spectroscopic properties of some cobalt, iron, ruthenium, and osmium complexes adsorbed on gold electrodes *via* the sulfur-based binding groups (thiols, thiophenes, thiocyanates, *etc.*) were reported.[7,8] (ii) Reactivity of a few iron and rhodium complexes toward

^{a}*Institut für Anorganische Chemie, RWTH Aachen University, Landoltweg 1, 52074 Aachen, Germany. E-mail: paul.koegerler@ac.rwth-aachen.de, kirill.monakhov@ac.rwth-aachen.de*
^{b}*Chemistry Department, Iowa State University, 1711 Gilman Hall, Ames, IA 50011, USA*
^{c}*Jülich-Aachen Research Alliance (JARA-FIT) and Peter Grünberg Institute (PGI-6), Forschungszentrum Jülich, 52425 Jülich, Germany*

This journal is © the Partner Organisations 2016

Inorg. Chem. Front., 2016, **3**, 523–531 | 523

thiolate-stabilised gold nanoparticles was discussed.[9] (iii) The mono- and dinuclear Cr(III)[10] and Ni(II)[11] complexes bearing thioether groups at the periphery of the PNP and PNP = S chelates were exploited for the catalytic polymerisation and oligomerisation of ethylene. (iv) In view of the high interest for the selective formation of self-assembly of highly ordered and oriented metal–organic monolayers on surfaces or the integration of metal complexes into mesoporous materials,[12] the deposition of S-terminated heterometallic complexes and clusters of Mo and Pd or Pt was studied on gold surfaces by scanning tunnelling microscopy (STM), ellipsometry, and X-ray photoelectron spectroscopy (XPS).[13] (v) The tetrahedral mixed-metal $\{RuCo_3\}$ carbonyl clusters functionalised with the phosphane–thiol ligands were studied on a gold surface by STM, XPS and X-ray absorption spectroscopy.[14] (vi) The chemical, structural, and thermodynamic characterisation of the mononuclear Pt(II) *cis*-complexes and the heterotrinuclear $\{Co_2Pt\}$ clusters containing *N*-substituted bis(diphenylphosphanyl) amine ligands with the pendant thiobenzyl ester groups[15] as well as a trinuclear Ag(I) complex and a Ag(I) coordination polymer with a thioether function in their short-bite diphosphine ligands[16] were described. (vii) Sulfur-assisted phenyl migration from phosphorus to platinum in molecular $\{PtW_2\}$ and $\{PtMo_2\}$ clusters with thioether-functionalised short-bite ligands of the bis(diphenylphosphanyl)amine-type was demonstrated.[17] The synthesis and structural chemistry of several methylthio- or thiocyanate-furnished coordination complexes of Mn(II,III),[18] Fe(II),[19] and Fe(III)[20] which exhibit ferromagnetic and antiferromagnetic exchange interactions were also reported. To the best of our knowledge, the potential of the above-mentioned metal complexes in catalytic processes on substrate surfaces has not been explored so far.

By contrast, surface studies towards nano and quantum computation which used the thioether-functionalised molecules exhibiting slow-relaxation of magnetisation (single-molecule magnets, SMMs) were performed and dealt with the $\{Mn_8^{III}Mn_4^{IV}\}$,[21] $\{Fe_4^{III}\}$[22] (see also gold nanoparticles functionalised with a 1,2-dithiolane-decorated Fe_4^{III} SMM[23]), $\{Fe_3^{III}Cr^{III}\}$,[24] and $\{Ni_4^{II}\}$[25] complexes. The chemical and physical behaviour of the $\{Cr_7^{III}Ni^{II}\}$-nuclearity rings[26] (with antiferromagnetic coupling in bulk) and the $\{Mn_{12}^{III}Mn_7^{II}\}$-nuclearity compound[27] (with ferromagnetic coupling in bulk) upon deposition and anchoring to gold surfaces *via* sulfur bonds was assessed.

Our exploratory work is motivated by the potential use of isolated transition metal coordination complexes and clusters with the structurally exposed sulfur-based anchoring groups in industrially relevant catalytic processes on solid supports at low and high temperatures. Our strategy implies the synthesis and characterisation of polynuclear metal compounds with the functional nano-sized structures as well as their addressing from the perspectives of homogeneous catalysis, with the subsequent immobilisation of these molecules onto porous metallic substrates or noble metal-coated mesoporous silica nanoparticles[28] (*e.g.*, SBA-15) to eventually enable supported-transition metal complex heterogeneous (or heterogenised homogeneous[29]) catalysis. In particular, Ni(II) Schiff-base complexes,[30] used as catalysts in the hydrogenation (see, *e.g.* reduction of benzene[31]) and oxidation reactions as well as for the ethylene polymerisation,[32] constitute interesting target candidates for the above-mentioned functionalisation and application.

Herein, we report the preparation of two novel polynuclear nickel(II) complexes supported by a π-conjugated Schiff-base ligand with the chemically engineered –SMe functionalities

Paul Kögerler graduated with a Dr rer. nat. degree with Prof. Achim Müller at the University of Bielefeld (Germany) in 2000, followed by a postdoctoral research stay at the Department of Physics and Astronomy at Iowa State University (USA). In 2003, he was appointed as a tenured Associate Scientist at the U.S. DOE Ames Laboratory, before returning to Germany in 2006 as Professor of Chemistry at the Institute of Inorganic Chemistry

Paul Kögerler

at RWTH Aachen University and Group Leader for Molecular Magnetism at the Peter Grünberg Institute, Research Centre Jülich.

Kirill Monakhov received his Dr rer. nat. degree with Prof. Gerald Linti at Heidelberg University (Germany) in 2010. After two years as a postdoctoral fellow of the German Research Foundation (DFG) and Cercle Gutenberg with Prof. Pierre Braunstein (University of Strasbourg, France), and after being awarded the Academia Europaea Burgen Scholarship in 2011, he returned to Germany in 2013 with a DFG postdoctoral reintegration fellow-
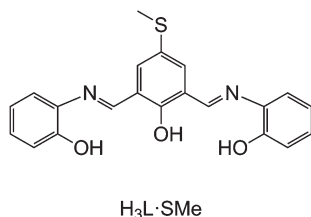
Kirill Yu. Monakhov

ship to join the group of Prof. Paul Kögerler at RWTH Aachen University. In 2015 he received a DFG Emmy Noether fellowship and now leads a junior research group at the Institute of Inorganic Chemistry at RWTH Aachen. His research interests include coordination and supramolecular chemistry, redox-active magnetic molecules, molecular electronics and spintronics, computational chemistry, catalysis and surface science.

524 | *Inorg. Chem. Front.*, 2016, **3**, 523–531

This journal is © the Partner Organisations 2016

Fig. 1 The hexadentate Schiff base $H_3L\cdot SMe$ ($=C_{21}H_{18}N_2O_3S$) used in this work.

(see $H_3L\cdot SMe$ in Fig. 1), isolated as $[Ni_6(L\cdot SMe)_3(CO_3)(MeOH)_6(THF)_2]Cl\cdot 2MeOH$ (**1**) and $[Ni_8(HL\cdot SMe)_2(L\cdot SMe)_2(OH)_4(MeCN)_4(H_2O)_4](NO_3)_2$ (**2**), which are of relevance to *in situ* ultra-high vacuum deposition on surfaces by electrospray ionisation[33] (ESI). The obtained ionic compounds were characterised by infrared (IR) spectroscopy, ESI mass spectrometry (ESI-MS), and thermogravimetric analysis (TGA) and their solid-state molecular structures were determined by single-crystal X-ray diffraction. The magnetic properties were assessed *via* dc and ac magnetic susceptibility measurements and our study thus expands knowledge on existing topologies and magnetism in nickel coordination chemistry.[34]

Results and discussion

Synthesis and thermal stability

Compounds **1** and **2** were synthesised *via* one-pot four-component *in situ* reactions of *n* equivalents of $NiX_2\cdot 6H_2O$ [*n* = 2 for X = Cl (**1**) and *n* = 1.4 for X = NO_3 (**2**)] with two equivalents of 2-aminophenol, one equivalent of freshly prepared 2-hydroxy-5-(methylthio)isophthalaldehyde and two equivalents of triethylamine under reflux conditions in a mixture of organic solvents (Scheme 1). Note that upon increasing *n* to 2 in the synthesis reaction for compound **2**, no solid product could be isolated. Likewise, changing or replacing the counteranions in the Ni(ɪɪ) precursors also prevents precipitation of crystalline product. A methanol/tetrahydrofuran volume ratio of 4 : 1 was used for the formation of the moisture stable, crys-

talline compound $[Ni_6(L\cdot SMe)_3(CO_3)(MeOH)_6(THF)_2]Cl\cdot 2MeOH$ (**1**) and a acetonitrile/benzonitrile volume ratio of 10 : 1 for the moisture sensitive, crystalline compound $[Ni_8(HL\cdot SMe)_2(L\cdot SMe)_2(OH)_4(MeCN)_4(H_2O)_4](NO_3)_2\cdot 11MeCN\cdot 2PhCN$ (**2**). The aerobic reaction affording compound **1** is furthermore characterised by the uptake of atmospheric CO_2. Dark-red compounds **1** and **2** with a potentially redox-active, fully-deprotonated $L\cdot SMe^{3-}$ ligand (see Fig. S1 and synthesis of $H_3L\cdot SMe$ in the ESI†) were obtained in *ca.* 39% and 55% yields, respectively. Compound **1** is well soluble in THF, DMF, and MeCN and modestly soluble in MeOH and CH_2Cl_2, while compound **2** is well soluble in THF, DMF, and MeOH and moderately soluble in MeCN and CH_2Cl_2.

In contrast to the gradual decomposition in TGA experiments of compound **2** occurring as an ill-defined mass loss step between 40 and 800 °C, the thermal stability of compound **1** in a N_2 atmosphere is characterised by three distinctive steps: (i) the first step (40–210 °C) corresponds to a 13.8% mass loss of two uncoordinated MeOH solvent molecules (the compound was measured immediately following synthesis) as well as two THF and two MeOH ligands coordinated to the Ni1/Ni'1 and Ni2/Ni'2 atoms, respectively (Δm_{calc} = 13.8%). (ii) The second step shows a 6.6% mass loss of four remaining MeOH ligands coordinated to the Ni3/Ni'3 atoms (Δm_{calc} = 6.5%) between 210 °C and 390 °C. (iii) The third, small step (1.8% mass loss from 390 °C to 400 °C) indicates chloride counterion desorption (Δm_{calc} = 1.8%). Thus, the TGA suggests that the $[Ni_6(L\cdot SMe)_3(CO_3)]^+$ core fragment is stable up to *ca.* 390 °C and this high thermal stability might enable the use of this magnetic complex in high-temperature catalytic reactions[32] on solid supports. It is noteworthy that the molecular ion peak of $[Ni_6(L\cdot SMe)_3(CO_3)H_2]^+$ without coordinated solvent molecules could be detected by ESI mass spectrometry (Fig. S7†).

Interestingly, the use of 2-hydroxy-5-methylisophthalaldehyde (see Fig. S2† for the structure of the non-functionalised H_3L ligand) instead of its methylthio derivate in the synthesis under less basic conditions (in the absence of Et_3N; Scheme S1†) has resulted in the formation of mononuclear nickel(ɪɪ) Schiff-base complexes with compositions $[Ni(H_3L)_2]Cl_2\cdot 4MeOH$ (**A**) and $[Ni(H_3L)_2](NO_3)_2\cdot 4MeOH$ (**B**), see
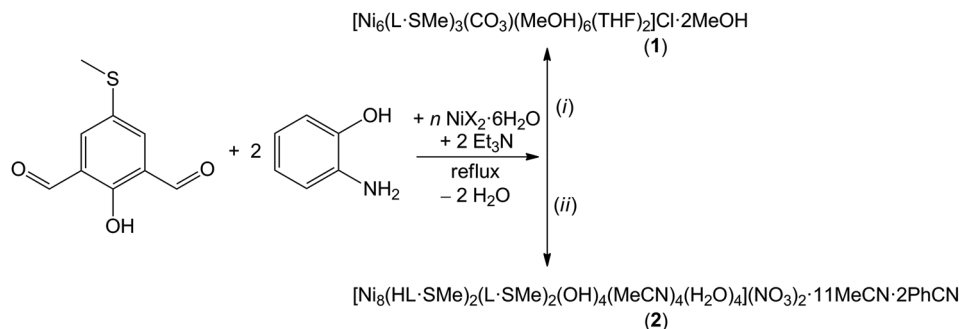
Scheme 1 Synthesis of the hexanuclear and octanuclear nickel(ɪɪ) Schiff-base complex compounds **1** and **2**. Reaction conditions: (i) *n* = 2 for X = Cl and MeOH : THF = 4 : 1; (ii) *n* = 1.4 for X = NO_3 and MeCN : PhCN = 10 : 1. For the IR spectra of these compounds, see Fig. S3 and S4.†

This journal is © the Partner Organisations 2016

Inorg. Chem. Front., 2016, **3**, 523–531 | **525**

Fig. S8 and Tables S5–S8† for solid-state structure information. The sulfur ligand constituents and the presence of triethylamine thus appear to be crucial for the synthesis of compounds **1** and **2**.

X-ray crystal structure analysis

The solid-state molecular structures of compounds **1** and **2** were established by single-crystal X-ray diffraction analyses and are illustrated in Fig. 2–4. Compound **1** crystallises in the monoclinic space group $P2/c$ (Table S1, the ESI†) and consists of the cationic complex $[Ni_6(L \cdot SMe)_3(CO_3)(MeOH)_6(THF)_2]^+$ (Fig. 2a), counterbalanced by a Cl^- anion, and two crystal solvent (methanol) molecules. The nano-sized $[Ni_6(L \cdot SMe)_3-(CO_3)(MeOH)_6(THF)_2]^+$ complex contains a distorted horseshoe-shaped Ni_6 core structure. The Ni atoms are connected to a μ_6-CO_3^{2-} group, a result of the fixation of atmospheric carbon dioxide (Fig. 2b). Molecular "horseshoe"-like structures have also been observed for $\{Cr_6^{III}\}$-nuclearity complexes.[35] Sorption of atmospheric CO_2 under aerobic reaction conditions is well-known in coordination chemistry;[36] homonuclear and heteronuclear transition-metal and lanthanide complexes that incorporate the carbonate ion in a wide variety of bridging modes have been described.[37]

The $\{CO_3 \subset Ni_6\}$ fragment in compound **1** is ligated by three *in situ*-formed Schiff bases (threefold-deprotonated $L \cdot SMe^{3-}$; see Fig. 1) acting as N_2O_3-chelates for the divalent nickel centres. Six MeOH and two THF solvent molecules complete the coordination spheres of metal ions (Fig. 3): Ni1 or Ni′1 site binds to one THF molecule, Ni2 or Ni′2 to one terminal MeOH molecule, and Ni3 or Ni′3 to two terminal MeOH molecules. Bond distances of the NO_5-coordinated nickel ions (in Å): Ni1–$O_{L \cdot SMe}$: 2.0010(19)–2.158(2) Å; Ni1–$N_{L \cdot SMe}$: 1.976(2) Å; Ni1–O_{THF}: 2.098(2) Å; Ni1–O_{CO_3}: 2.0896(19); Ni2–$O_{L \cdot SMe}$: 1.9726(18)–2.143(2); Ni2–$N_{L \cdot SMe}$: 1.963(2); Ni2–O_{MeOH}: 2.119(2); Ni2–O_{CO_3}: 2.0306(18); Ni3–$O_{L \cdot SMe}$: 2.000(2) and 2.0359(19); Ni3–$N_{L \cdot SMe}$: 1.995(2); Ni3–O_{MeOH}: 2.095(2) and 2.112(2); Ni3–O_{CO_3}: 2.0856(19). Thus, each Ni(II) centre in compound **1** exhibits a pseudo-octahedral local geometry with axially distorted O positions. The $[Ni_6(L \cdot SMe)_3(CO_3)(MeOH)_6(THF)_2]^+$ structure reveals the non-bonding Ni1⋯Ni2 (or Ni′1⋯Ni′2), Ni1⋯Ni3 (or Ni′1⋯Ni′3), and Ni2⋯Ni′2 separations of 2.9707(6), 3.1251(6), and 3.0323(7) Å, respectively (the sum of the covalent radii of two Ni atoms is 2.48 Å (ref. 38)). The magnetically relevant bond angles fall in the ranges 90.313(74)–90.828(78)° for Ni1–$(\mu_3$-O)–Ni2, 96.916(79)–101.451(84)° for Ni1–$(\mu_3$-O)–Ni3, and 96.608(17)–100.461(17)° for Ni2–$(\mu_3$-O)–Ni′2.
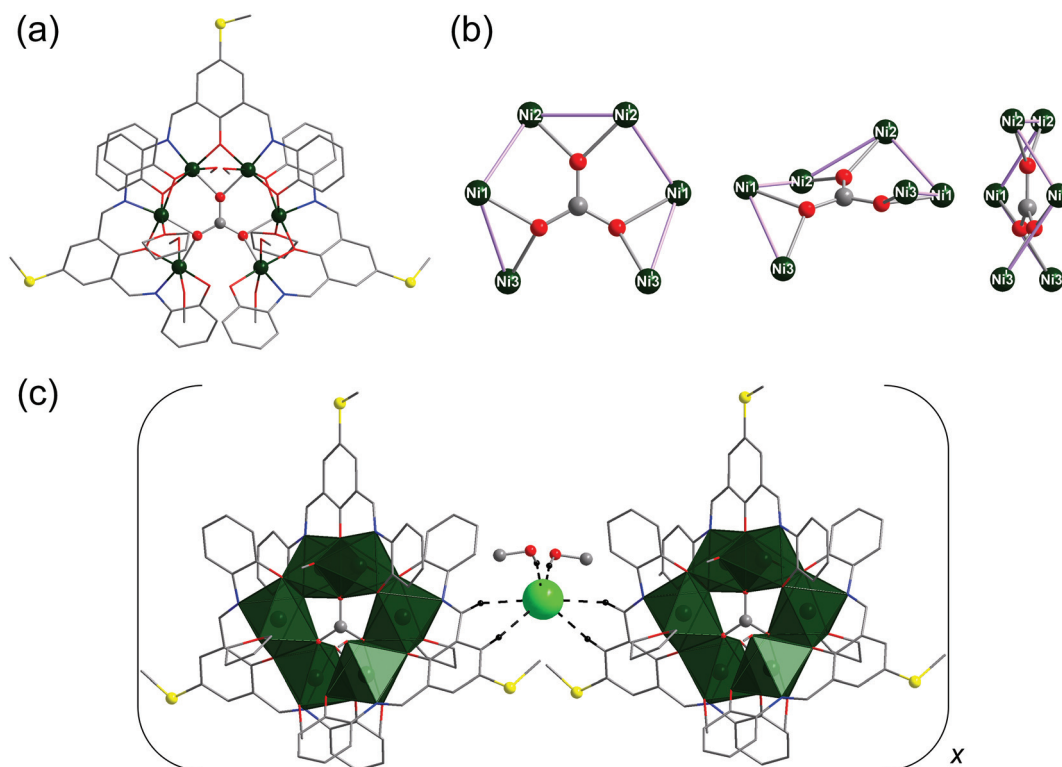
Fig. 2 (a) Molecular structure of $[Ni_6(L \cdot SMe)_3(CO_3)(MeOH)_6(THF)_2]^+$ in compound **1**. (b) Different views of the Ni_6 core templated by CO_3^{2-} with a μ_6-η^1:η^1:η^1:η^1:η^1:η^1 binding mode. (c) A segment of the extended solid-state structure of compound **1**, highlighting the association of two $\{Ni_6\}$ coordination clusters *via* C–$H_{L \cdot SMe}$⋯Cl hydrogen bonding interactions (O–H_{MeOH}⋯Cl interactions are also shown). Hydrogen atoms not involved in hydrogen bonds are omitted for clarity. Colour code: H, black; C, grey; N, blue; O, red; S, yellow; Cl, light green; Ni, dark green. The nickel and sulfur atoms, carbonate ion, and co-crystallised MeOH molecules are represented as ball-and-stick models. The chloride ion is depicted as space-filling model. See Table S2† for bond lengths and angles.
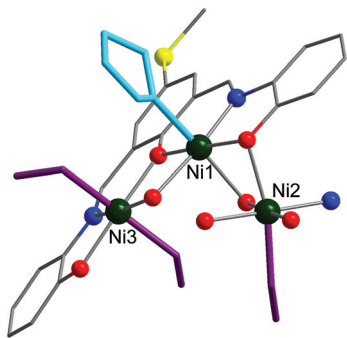
526 | *Inorg. Chem. Front.*, 2016, **3**, 523–531

This journal is © the Partner Organisations 2016

Fig. 3 A fragment of compound **1** representing pseudo-octahedral coordination geometries of the Ni(II) centres. For clarity, only one chelating Schiff-base ligand L·SMe^{3-} is explicitly depicted. The nickel, nitrogen, oxygen, and sulfur atoms are represented as ball-and-stick models. The terminal-coordinated solvent molecules are highlighted in different colours: MeOH, purple; THF, sky blue. Elemental colour code: C, grey; N, blue; O, red; S, yellow; Ni, dark green.
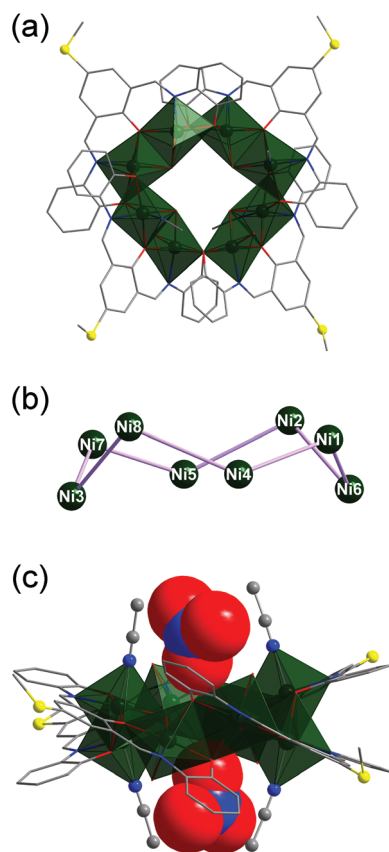

Fig. 4 (a) Molecular structure of [Ni$_8$(HL·SMe)$_2$(L·SMe)$_2$(OH)$_4$-(MeCN)$_4$(H$_2$O)$_4$]$^{2+}$ in compound **2**. (b) Non-planar ring of eight nickel(II) atoms as metal core in compound **2**. (c) Side view of the solid-state structure of compound **2** showing two NO$_3^-$ anions in the top and down cavities. Hydrogen atoms and solvent molecules are omitted for clarity. The nickel and sulfur atoms as well as the C and N atoms of MeCN in (c) are represented as ball-and-stick models and the nitrate ions as space-filling models. Colour code: C, grey; N, blue; O, red; S, yellow; Ni, dark green. See Table S4† for bond lengths and angles.

A further interesting feature of compound **1** is the infinite one-dimensional chain structure in the crystal lattice, made up from repeating [Ni$_6$(L·SMe)$_3$(CO$_3$)(MeOH)$_6$(THF)$_2$]$^+$ entites assembled via four C–H$_{L·SMe}$···Cl ($d_{C···Cl}$ = 3.6385(4) Å and 3.7100(4) Å) and two identical O–H$_{MeOH}$···Cl ($d_{O···Cl}$ = 3.0958(3) Å) hydrogen bonds, as shown in Fig. 2c.

Compound **2** crystallises in the triclinic space group P$\bar{1}$ (Table S3†) and shows a dicationic {Ni$_8$} metallamacrocycle [Ni$_8$(HL·SMe)$_2$(L·SMe)$_2$(OH)$_4$(MeCN)$_4$(H$_2$O)$_4$]$^{2+}$ (Fig. 4a), reminiscent of a rollercoaster, and counterbalanced by two NO$_3^-$ anions. Eleven acetonitrile and two benzonitrile molecules co-crystallise in the unit cell. The central metal core in the nano-sized [Ni$_8$(HL·SMe)$_2$(L·SMe)$_2$(OH)$_4$(MeCN)$_4$(H$_2$O)$_4$]$^{2+}$ moiety displays a non-planar ring of eight nickel(II) atoms (Fig. 4b). This ring is maintained by two monoprotonated HL·SMe^{2-} and two fully-deprotonated L·SMe^{3-} Schiff-base ligands (see Fig. 1) as well as four bridging OH$^-$ groups. The coordination spheres of four nickel (Ni2, Ni3, Ni6 and Ni8) atoms are completed by terminal MeCN molecules, those of the other four (Ni1, Ni4, Ni5 and Ni7) only by terminal H$_2$O molecules (one MeCN/H$_2$O per Ni). As a result, each of the Ni(II) ions in the ring resides in a pseudo-octahedral N$_2$O$_4$ or NO$_5$ coordination environment (ratio N$_2$O$_4$: NO$_5$ = 4 : 4). The NiN$_2$O$_4$ bond distances (in Å) amount to Ni2–O$_{L·SMe}$: 1.990(7)–2.151(7); Ni2–N$_{L·SMe}$: 1.980(8); Ni2–OH: 2.045(7), Ni2–N$_{MeCN}$: 2.091(8); Ni3–O$_{L·SMe}$: 1.973(7)–2.171(7); Ni3–N$_{L·SMe}$: 1.992(9), Ni3–OH: 2.061(7); Ni3–N$_{MeCN}$: 2.075(10); Ni6–O$_{L·SMe}$: 1.978(7)–2.162(7); Ni6–N$_{L·SMe}$: 1.992(8); Ni6–OH: 2.029(7); Ni6–N$_{MeCN}$: 2.112(9); Ni8–O$_{L·SMe}$: 1.996(7)–2.141(7); Ni8–N$_{L·SMe}$: 1.977(9), Ni8–OH: 2.056(7), Ni8–N$_{MeCN}$: 2.080(10). For the NiNO$_5$ environment: Ni1–O$_{L·SMe}$: 2.027(7)–2.087(7); Ni1–N$_{L·SMe}$: 2.013(8); Ni1–OH: 2.093(7), Ni1–O$_{H_2O}$: 2.071(7); Ni4–O$_{L·SMe}$: 2.039(7)–2.077(7); Ni4–N$_{L·SMe}$: 2.018(9); Ni4–OH: 2.138(6); Ni4–O$_{H_2O}$: 2.059(7); Ni5–O$_{L·SMe}$: 2.038(7)–2.054(7); Ni5–N$_{L·SMe}$: 2.010(8), Ni5–OH: 2.133(7); Ni5–O$_{H_2O}$: 2.071(7); Ni7–O$_{L·SMe}$: 2.043(7)–2.063(7); Ni7–N$_{L·SMe}$: 1.991(8); Ni7–OH: 2.116(7); Ni7–O$_{H_2O}$: 2.080(8). The non-equivalent, non-bonding Ni···Ni distances range from 3.0662(25) to 3.1001(25) Å. The magnetically relevant bond angles fall in the ranges 93.5(3)–100.7(3)° for Ni3–(μ$_3$-O20$_{L·SMe}$)–Ni8 and Ni3–(μ$_3$-O12$_{L·SMe}$)–Ni7, and 95.1(3)–96.6(3)° for Ni2–(μ$_2$-O14$_{OH}$)–Ni5 and Ni1–(μ$_2$-O15$_{OH}$)–Ni6.

In general, the [Ni$_8$(HL·SMe)$_2$(L·SMe)$_2$(OH)$_4$(MeCN)$_4$-(H$_2$O)$_4$]$^{2+}$ architecture can be viewed as a metallocavitand[39] hosting two NO$_3^-$ anions in a nesting fashion (Fig. 4c). These nitrate groups are situated 2.3973(80) Å above and 2.6004(83) Å below the nickel ring plane and connected to the internal oxygen atoms of the dicationic complex via four H-bonds: (i) O21 or O26 of NO$_3^-$ is linked to two bridging OH$^-$ groups (O21–O$_{OH}$: 2.7958(123) Å–2.8692(117) Å; O26–O$_{OH}$: 2.9280(101) Å–2.9428(123) Å) and one coordinated H$_2$O molecule (O21–O5$_{H_2O}$: 3.0352(115) Å; O26–O9$_{H_2O}$: 2.9195(145) Å). (ii) The fourth H-bond appears between O22 or O25 of NO$_3^-$ and the H$_2$O ligands at the Ni1 and Ni4 centres (O22–O7$_{H_2O}$: 2.7542(125) Å; O25–O6$_{H_2O}$: 2.8609(123) Å).

We note that in the crystal structures of compounds **1** and **2**, the S atoms at the periphery of the Schiff-base ligands

This journal is © the Partner Organisations 2016

Inorg. Chem. Front., 2016, **3**, 523–531 | **527**

$L \cdot SMe^{3-}$ and $HL \cdot SMe^{2-}$ are not involved in any intermolecular coordination bonds.

Magnetism and magnetochemical modelling

Magnetic properties of compounds **1** and **2** were studied based on the temperature- and field-dependent dc (static) and ac (dynamic) magnetic susceptibility. Since the ac susceptibilities do not reveal any out-of-phase components for compounds **1** nor **2**, the experimental data of the magnetic dc measurements are presented as $\chi_m T$ vs. T and M_m vs. B curves in Fig. 5. For compound **1**, a $\chi_m T$ value of 7.68 cm³ K mol⁻¹ at 290 K is within the interval of 5.88–9.19 cm³ K mol⁻¹ expected for six non-interacting high-spin Ni(II) centres.[40] Lowering the temperature, $\chi_m T$ slowly decreases for $T > 100$ K and rapidly decreases below that point indicating predominantly antiferromagnetic exchange interactions between the Ni(II) centres. For compound **2**, the corresponding value at 290 K is 9.29 cm³ K mol⁻¹ being in the range expected for eight non-interacting high-spin Ni(II) centres (7.84–12.25 cm³ K mol⁻¹).[40] In contrast to compound **1**, $\chi_m T$ slowly increases by decreasing the temperature, reaching a maximum at $T \approx 30$ K. The $\chi_m T$ value rapidly decreases on further temperature decrease. Such a maximum results from predominantly ferromagnetic exchange interactions between the eight Ni(II) centres. Since both magnetisation curves of compounds **1** and **2** do not exhibit saturation, a reliable conclusion with respect to the upper limit of total effective spin ground state S_{tot} is impossible.

A model description of the magnetic susceptibilities was based on the following assumptions, in order to contain computational limitations and to restrict the number of independent fitting parameters: Since the ligand field of each Ni(II) centre is well approximated as octahedrally symmetric, the ground term is an orbital momentum singlet $^3A_2$ originating from ground term ^3F of the free high-spin Ni(II) ion – according to the crystal structure, the distortion of the octahedral

symmetry is expected to be small. Therefore, the zero-field splitting is expected to be negligible and thus omitted. Hence, the magnetic features of compounds **1** and **2** are described in terms of an isotropic effective spin approach ($S = 1$) including an effective Heisenberg-Hamiltonian to characterise the exchange interactions. The number of exchange parameters is restricted in a further approximation: exchange pathways exhibiting similar geometries are assumed as identical, see Fig. 6 for the resulting coupling schemes.

The exchange interaction Hamiltonian for compound **1**

$$\hat{H}_{ex,1} = -2J_A(\hat{S}_1\hat{S}_2 + \hat{S}_5\hat{S}_6) - 2J_B(\hat{S}_2\hat{S}_3 + \hat{S}_4\hat{S}_5) - 2J_C\hat{S}_3\hat{S}_4$$

and accordingly for compound **2**

$$\hat{H}_{ex,2} = -2J_A(\hat{S}_1\hat{S}_2 + \hat{S}_5\hat{S}_6) - 2J_B(\hat{S}_2\hat{S}_3 + \hat{S}_4\hat{S}_5)$$
$$- 2J_C(\hat{S}_6\hat{S}_7 + \hat{S}_1\hat{S}_8) - 2J_D\hat{S}_7\hat{S}_8 - 2J_E\hat{S}_3\hat{S}_4$$

in combination with the Zeeman Hamiltonian are employed to model the experimental data within the computational framework CONDON 2.0.[41] The least-squares fit to the magnetic data of compound **1** (quality-of-fit parameter SQ = 0.9%) results in the exchange parameters $J_A = -7.7 \pm 0.1$ cm⁻¹, $J_B = +7.2 \pm 0.1$ cm⁻¹, $J_C = -2.6 \pm 0.1$ cm⁻¹, and an isotropic g-value of $g_{iso} = 2.25 \pm 0.01$. These parameters confirm the predominantly antiferromagnetic exchange interaction between the six Ni(II) centres. The magnitudes of the exchange interaction energies reveal weak interactions within the compound that result in a ground state of a total effective spin $S_{tot} = 0$.

The least-squares fit to the magnetic susceptibility data of compound **2** is slightly worse (SQ = 1.5%) if a model including three independent exchange coupling parameters ($J_A = J_D = -1.6 \pm 0.1$ cm⁻¹, $J_B = -1.2 \pm 0.1$ cm⁻¹, $J_C = J_E = +5.2 \pm 0.1$ cm⁻¹, $g_{iso} = 2.13 \pm 0.02$) is employed. A slightly better goodness-of-fit is achieved (SQ = 1.2%) in the approximation shown in Fig. 6 based on the less-symmetric structure of the compound, although the margin of error of the fit parameter J_E is larger. The corresponding least-squares parameters are $J_A = -1.5 \pm 0.2$ cm⁻¹, $J_B = -1.1 \pm 0.1$ cm⁻¹, $J_C = +4.6 \pm 0.1$ cm⁻¹, $J_D = -1.6 \pm 0.1$ cm⁻¹, $J_E = +4.9 \pm 1.7$ cm⁻¹ and $g_{iso} = 2.13 \pm 0.02$. Even though the calculated values exhibit weaker net exchange interactions in compound **2** than in compound **1**, they confirm the predominantly ferromagnetic interaction between the eight Ni(II) centres. According to the calculated parameters,
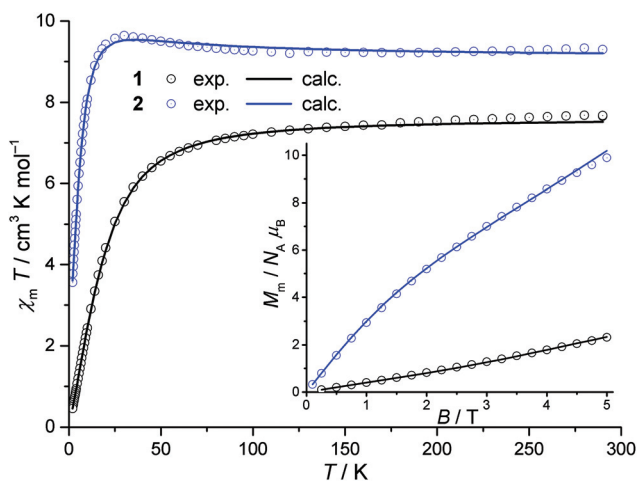

Fig. 5 Temperature dependence of $\chi_m T$ at 0.1 Tesla for compounds **1** and **2**; inset: field dependence of the molar magnetisation M_m at 2 K; circles: experimental data, solid graphs: least-squares fits.
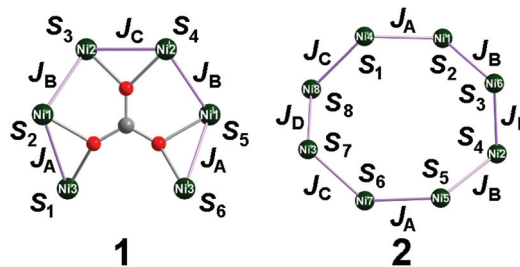

Fig. 6 Coupling schemes used for the magnetochemical modelling for compounds **1** and **2**.

the ground state of compound **2** is characterised by a total effective spin $S_{tot} = 2$.

Conclusion

We synthesised and characterised two polynuclear nickel(II) compounds **1** and **2** with structurally exposed thioether functional groups in the periphery of the cationic complexes $[Ni_6(L \cdot SMe)_3(CO_3)(MeOH)_6(THF)_2]^+$ and $[Ni_8(HL \cdot SMe)_2(L \cdot SMe)_2(OH)_4(MeCN)_4(H_2O)_4]^{2+}$, respectively. These coordination clusters with distinct nickel topologies are characterised by different total ground-state spins and exhibit different types of exchange interactions: predominantly antiferromagnetic for the horseshoe-like {Ni$_6$} with $S_{tot} = 0$ and predominantly ferromagnetic for the rollercoaster-like {Ni$_8$} with $S_{tot} = 2$. Due to specific chemical properties (thermal stability, solubility and detectability following ESI-MS), the anion-templated self-assembly **1** appears to be a suitable candidate for molecular deposition and anchoring onto metallic surfaces *via* a thioether linkage and studies at solid–liquid interfaces. In forthcoming studies we will explore its potential as a heterogenised homogeneous catalyst, for example *via* the use of cation exchange[42] to incorporate the solvent-free $[Ni_6(L \cdot SMe)_3(CO_3)]^+$ fragment into large-pore metal–organic frameworks. We also plan to assess compound **1** and its carbonate-bonded metal core $[Ni_6(L \cdot SMe)_3(CO_3)]^+$ as catalysts for ethylene oligomerisation where we expect the catalytic activity and selectivity to also depend on the pendant thioether groups.[11b,c,43] Finally, we target the immobilisation of the horseshoe-like {Ni$_6$} complex with its structurally exposed thioether anchoring groups onto noble metal-coated mesoporous silica nanoparticles (such as SBA-15),[44] in order to probe industrially relevant catalytic oxidation reactions on solid supports at low and high temperatures.

Experimental

Materials and methods

The synthesis of compounds **1**, **2**, **A** and **B** was carried out under aerobic conditions. All starting materials were from commercial sources and used as received. Solvents were used without further purification. The IR spectra of compounds **1**, **2**, **A** and **B** were recorded on a Nicolet Avatar 360 FTIR spectrometer (KBr pellets, ν = 4000–400 cm^{-1}). TG/DT analyses of compounds **1** and **2** were performed under N$_2$ flow and a heating rate of 5 K min^{-1} in the temperature range 25–800 °C on a Mettler Toledo TGA/SDTA 851e instrument. The ESI-MS spectrum of compound **1** in the positive ion mode was recorded on a 4000 QTRAP mass spectrometer system, using the LC/LC-MS method with direct infusion.

Synthesis of $[Ni_6(L \cdot SMe)_3(CO_3)(MeOH)_6(THF)_2]Cl \cdot 2MeOH$ (1). NiCl$_2 \cdot$6H$_2$O (0.095 g, 0.4 mmol), 2-hydroxy-5-(methylthio)isophthalaldehyde (0.040 g, 0.2 mmol) and 2-aminophenol (0.044 g, 0.4 mmol) were solved in a mixture of MeOH (8 mL),

THF (2 mL) and triethylamine (0.056 mL, 0.4 mmol). The resulting red coloured mixture was stirred for 90 minutes under reflux. The MeOH/THF/Et$_3$N solution was filtered off and the filtrate was kept in a capped vial at room temperature. Dark-red single crystals of compound **1** were obtained *via* slow evaporation after *ca.* two weeks and then washed with a small amount of ice-cold methanol. Yield of the air-dried crystals: 0.049 g (38.5% based on H$_3$L). C$_{78}$ClH$_{85}$N$_6$Ni$_6$O$_{20}$S$_3$ (1910.34 g mol^{-1}; disregarding solvent). IR (KBr pellet), ν_{max}/cm^{-1}: 3405 (br,m), 2919 (w), 1615 (m), 1586 (sh), 1524 (m), 1473 (s), 1456 (sh), 1431 (sh), 1389 (s), 1336 (sh), 1313 (m), 1256 (sh), 1187 (w), 1150 (w), 1109 (w), 1047 (m), 1035 (sh), 950 (w), 883 (w), 827 (w), 744 (m), 684 (w), 589 (w), 524 (m). MS (MeOH, $^+$ESI): *m/z*: 1536.8 (C$_{64}$H$_{47}$N$_6$Ni$_6$O$_{12}$S$_3$$^+$, 100%).

Synthesis of $[Ni_8(HL \cdot SMe)_2(L \cdot SMe)_2(OH)_4(MeCN)_4(H_2O)_4]$ (NO$_3$)$_2 \cdot$11MeCN$\cdot$2PhCN (2). Ni(NO$_3$)$_2 \cdot$6H$_2$O (0.060 g, 0.2 mmol), 2-hydroxy-5-(methylthio)isophthalaldehyde (0.040 g, 0.2 mmol) and 2-aminophenol (0.044 g, 0.4 mmol) were solved in a mixture of acetonitrile (10 mL), benzonitrile (1 mL) and triethylamine (0.056 mL, 0.4 mmol). The resulting red coloured mixture was stirred for 70 minutes under reflux. The MeCN/PhCN/Et$_3$N solution was filtered off and the filtrate was kept in a capped vial at room temperature. Red single crystals of compound **2** were obtained *via* slow evaporation after *ca.* one week and then washed with a small amount of ice-cold acetonitrile. Yield of the air-dried crystals: 0.033 g (55% based on Ni). C$_{92}$H$_{86}$N$_{14}$Ni$_8$O$_{26}$S$_4$ (2401.55 g mol^{-1}; disregarding solvent). IR (KBr pellet), ν_{max}/cm^{-1}: 3424 (br, m), 3056 (w), 2918 (w), 2224 (w), 1617 (s), 1587 (s), 1527 (s), 1478 (vs), 1457 (sh), 1434 (w), 1386 (vs), 1312 (s), 1292 (sh), 1278 (sh), 1252 (s), 1189 (w), 1150 (w), 1109 (w), 1051 (s), 953 (w), 882 (m), 827 (m), 748 (s), 687 (m), 589 (m), 549 (w), 517 (m).

X-ray crystallography

Single-crystal X-ray diffraction data for all compounds were collected on a Bruker Apex II diffractometer with Mo Kα radiation (λ = 0.71073 Å) at 153 K. Crystals were mounted in a Hampton cryoloop with Paratone-N oil. Absorption corrections were applied numerically based on multifaceted crystal model using SADABS software.[45] A summary of the crystal data and structure refinements for compounds **1**, **2**, **A** and **B** are given in Tables S1, S3, S5 and S7 in the ESI,† respectively. Details are described in the CIF files. CCDC 1440001–1440004 contain the supplementary crystallographic data for this paper.

Magnetic susceptibility measurements

Magnetic susceptibility data of compounds **1** and **2** were recorded using a Quantum Design MPMS-5XL SQUID magnetometer for direct current (dc) and alternating current (ac) measurements. The polycrystalline samples were compacted and immobilised into cylindrical PTFE capsules. The dc susceptibility data were acquired as a function of the field (0.1–5.0 T) and temperature (2.0–290 K). The ac susceptibility data were measured in the absence of a static bias field in the 10–1000 Hz frequency range (T = 2.0–50 K, B_{ac} = 3 G), but no out-of-phase signals were detected. Data were corrected for dia-

This journal is © the Partner Organisations 2016

Inorg. Chem. Front., 2016, **3**, 523–531 | **529**

magnetic contributions from the sample holder and the compounds ($\chi_{dia}(\mathbf{1}) = -0.96 \times 10^{-3}$ cm^3 mol^{-1}, $\chi_{dia}(\mathbf{2})$: -1.20×10^{-3} cm^3 mol^{-1}).

Acknowledgements

References

1 M. N. Rittner, *J. of Metals*, 2004, **56**, 22.

2 *Modern Surface Organometallic Chemistry*, ed. J.-M. Basset, R. Psaro, D. Roberto and R. Ugo, Wiley-VCH, Weinheim, 2009.

3 L. Bogani and W. Wernsdorfer, *Nat. Mater.*, 2008, **7**, 179.

4 See, *e.g.*: (*a*) I. S. Kristensen, D. J. Mowbray, K. S. Thygesen and K. W. Jacobsen, *J. Phys.: Condens. Matter*, 2008, **20**, 374101; (*b*) Z. Li, M. Smeu, M. A. Ratner and E. Borguet, *J. Phys. Chem. C*, 2013, **117**, 14890; (*c*) V. Kaliginedi, A. V. Rudnev, P. Moreno-García, M. Baghernejad, C. Huang, W. Hong and T. Wandlowski, *Phys. Chem. Chem. Phys.*, 2014, **16**, 23529. See also: (*d*) S. Schmitz, J. van Leusen, A. Ellern, P. Kögerler and K. Yu. Monakhov, *Inorg. Chem. Front.*, 2015, **2**, 1095.

5 A. Cornia, M. Mannini, P. Sainctavit and R. Sessoli, *Chem. Soc. Rev.*, 2011, **40**, 3076.

6 J. J. Parks, A. R. Champagne, T. A. Costi, W. W. Shum, A. N. Pasupathy, E. Neuscamman, S. Flores-Torres, P. S. Cornaglia, A. A. Aligia, C. A. Balseiro, G. K.-L. Chan, H. D. Abruña and D. C. Ralph, *Science*, 2010, **328**, 1370.

7 (*a*) T. T. T. Li, H. Y. Liu and M. J. Weaver, *J. Am. Chem. Soc.*, 1984, **106**, 1233; (*b*) K. I. Ozoemena, T. Nyokong and P. Westbroek, *Electroanalysis*, 2003, **15**, 1762; (*c*) W. Zhou, S. Ye, M. Abe, T. Nishida, K. Uosaki, M. Osawa and Y. Sasaki, *Chem. – Eur. J.*, 2005, **11**, 5040.

8 (*a*) H. O. Finklea and D. D. Hanshew, *J. Am. Chem. Soc.*, 1992, **114**, 3173; (*b*) M. S. Ravenscroft and H. O. Finklea, *J. Phys. Chem.*, 1994, **98**, 3843; (*c*) H. O. Finklea and M. S. Ravenscroft, *Isr. J. Chem.*, 1997, **37**, 179; (*d*) D. A. Brevnov and H. O. Finklea, *J. Electrochem. Soc.*, 2000, **147**, 3461; (*e*) R. M. Haddox and H. O. Finklea, *J. Phys. Chem. B*, 2004, **108**, 1694; (*f*) N. Tuccitto, V. Torrisi, M. Cavazzini, T. Morotti, F. Puntoriero, S. Quici, S. Campagna and A. Licciardello, *ChemPhysChem*, 2007, **8**, 227.

9 (*a*) M. Yamada and H. Nishihara, *Langmuir*, 2003, **19**, 8050; (*b*) M. Yamada, T. Tadera, K. Kubo and H. Nishihara, *J. Phys. Chem. B*, 2003, **107**, 3703; (*c*) T. Belser, M. Stoehr and A. Pfaltz, *J. Am. Chem. Soc.*, 2005, **127**, 8720.

10 Z. Weng, S. Teo and T. S. A. Hor, *Dalton Trans.*, 2007, 3493.

11 (*a*) K. Song, H. Gao, F. Liu, J. Pan, L. Guo, S. Zai and Q. Wu, *Eur. J. Inorg. Chem.*, 2009, 3016; (*b*) A. Ghisolfi, C. Fliedel, V. Rosa, R. Pattacini, A. Thibon, K. Yu. Monakhov and P. Braunstein, *Chem. – Asian J.*, 2013, **8**, 1795; (*c*) A. Ghisolfi, C. Fliedel, V. Rosa, K. Yu. Monakhov and P. Braunstein, *Organometallics*, 2014, **33**, 2523.

12 P. Van Der Voort, C. Vercaemst, D. Schaubroeck and F. Verpoort, *Phys. Chem. Chem. Phys.*, 2008, **10**, 347.

13 P. Croizat, F. Müller, H. Mantz, A. Englisch, R. Welter, S. Hüfner and P. Braunstein, *C. R. Chim.*, 2009, **12**, 1228.

14 A. Naitabdi, O. Toulemonde, J. P. Bucher, J. Rosé, P. Braunstein, R. Welter and M. Drillon, *Chem. – Eur. J.*, 2008, **14**, 2355.

15 V. Gallo, P. Mastrorilli, C. F. Nobile, P. Braunstein and U. Englert, *Dalton Trans.*, 2006, 2342.

16 V. Rosa, C. Fliedel, A. Ghisolfi, R. Pattacini, T. Avilés and P. Braunstein, *Dalton Trans.*, 2013, **42**, 12109.

17 S. Todisco, P. Mastrorilli, M. Latronico, V. Gallo, U. Englert, N. Re, F. Creati and P. Braunstein, *Inorg. Chem.*, 2015, **54**, 4777.

18 S. Mameri, A. M. Ako, F. Yesil, M. Hibert, Y. Lan, C. E. Anson and A. K. Powell, *Eur. J. Inorg. Chem.*, 2014, 4326.

19 C. Fliedel, V. Rosa, A. Falceto, P. Rosa, S. Alvarez and P. Braunstein, *Inorg. Chem.*, 2015, **54**, 6547.

20 A. Abhervé, J. M. Clemente-Juan, M. Clemente-León, E. Coronado, J. Boonmak and S. Youngme, *New J. Chem.*, 2014, **38**, 2105.

21 (*a*) A. Cornia, A. C. Fabretti, M. Pacchioni, L. Zobbi, D. Bonacchi, A. Caneschi, D. Gatteschi, R. Biagi, U. Del Pennino, V. De Renzi, L. Gurevich and H. S. J. Van der Zant, *Angew. Chem., Int. Ed.*, 2003, **42**, 1645; (*b*) L. Zobbi, M. Mannini, M. Pacchioni, G. Chastanet, D. Bonacchi, C. Zanardi, R. Biagi, U. Del Pennino, D. Gatteschi, A. Cornia and R. Sessoli, *Chem. Commun.*, 2005, 1640; (*c*) S. Voss, M. Burgert, M. Fonin, U. Groth and U. Rüdiger, *Dalton Trans.*, 2008, 499.

22 (*a*) M. Mannini, F. Pineider, P. Sainctavit, C. Danieli, E. Otero, C. Sciancalepore, A. M. Talarico, M.-A. Arrio, A. Cornia, D. Gatteschi and R. Sessoli, *Nat. Mater.*, 2009, **8**, 194; (*b*) F. Pineider, M. Mannini, C. Danieli, L. Armelao, F. M. Piras, A. Magnani, A. Cornia and R. Sessoli, *J. Mater. Chem.*, 2010, **20**, 187; (*c*) M. Mannini, F. Pineider, C. Danieli, F. Totti, L. Sorace, Ph. Sainctavit, M.-A. Arrio, E. Otero, L. Joly, J. Criginski Cesar, A. Cornia and R. Sessoli, *Nature*, 2010, **468**, 417; (*d*) M. Jesus Rodriguez-Douton, M. Mannini, L. Armelao, A.-L. Barra, E. Tancini, R. Sessoli and A. Cornia, *Chem. Commun.*, 2011, **47**, 1467.

23 M. Perfetti, F. Pineider, L. Poggini, E. Otero, M. Mannini, L. Sorace, C. Sangregorio, A. Cornia and R. Sessoli, *Small*, 2014, **10**, 323.

24 M. Mannini, E. Tancini, L. Sorace, P. Sainctavit, M.-A. Arrio, Y. Qian, E. Otero, D. Chiappe, L. Margheriti, J. C. Cezar, R. Sessoli and A. Cornia, *Inorg. Chem.*, 2011, **50**, 2911.

25 (*a*) A. Ghisolfi, K. Yu. Monakhov, R. Pattacini, P. Braunstein, X. López, C. de Graaf, M. Speldrich, J. van Leusen, H. Schilder and P. Kögerler, *Dalton Trans.*, 2014, **43**, 7847;

530 | *Inorg. Chem. Front.*, 2016, **3**, 523–531

This journal is © the Partner Organisations 2016

(b) V. Heβ, F. Matthes, D. E. Bürgler, K. Yu. Monakhov, C. Besson, P. Kögerler, A. Ghisolfi, P. Braunstein and C. M. Schneider, *Surf. Sci.*, 2015, **641**, 210.

26 (a) V. Corradini, R. Biagi, U. del Pennino, V. De Renzi, A. Gambardella, M. Affronte, C. A. Muryn, G. A. Timco and R. E. P. Winpenny, *Inorg. Chem.*, 2007, **46**, 4937; (b) V. Corradini, F. Moro, R. Biagi, V. De Renzi, U. del Pennino, V. Bellini, S. Carretta, P. Santini, V. A. Milway, G. Timco, R. E. P. Winpenny and M. Affronte, *Phys. Rev. B: Condens. Matter*, 2009, **79**, 144419; (c) V. Corradini, A. Ghirri, U. del Pennino, R. Biagi, V. A. Milway, G. Timco, F. Tuna, R. E. P. Winpenny and M. Affronte, *Dalton Trans.*, 2010, **39**, 4928; (d) H. Rath, G. A. Timco, V. Corradini, A. Ghirri, U. del Pennino, A. Fernandez, R. G. Pritchard, C. A. Muryn, M. Affronte and R. E. P. Winpenny, *Chem. Commun.*, 2013, **49**, 3404.

27 J. Dreiser, A. M. Ako, C. Wäckerlin, J. Heidler, C. E. Anson, A. K. Powell, C. Piamonteze, F. Nolting, S. Rusponi and H. Brune, *J. Phys. Chem. C*, 2015, **119**, 3550.

28 N. Song and Y.-W. Yang, *Chem. Soc. Rev.*, 2015, **44**, 3474.

29 M. G. L. Petrucci and A. K. Kakkar, *Adv. Mater.*, 1996, **8**, 251.

30 A. R. Silva, C. Freire, B. de Castro, M. M. A. Freitas and J. L. Figueiredo, *Microporous Mesoporous Mater.*, 2001, **46**, 211 and references cited therein.

31 V. Arun, N. Sridevi, P. P. Robinson, S. Manju and K. K. M. Yusuff, *J. Mol. Catal. A: Chem.*, 2009, **304**, 191.

32 K. C. Gupta and A. K. Sutar, *Coord. Chem. Rev.*, 2008, **252**, 1420 and references cited therein.

33 C. Hamann, R. Woltmann, I.-Po Hong, N. Hauptmann, S. Karan and R. Berndt, *Rev. Sci. Instrum.*, 2011, **82**, 033903.

34 For recent studies, see *e.g.*: (a) J. Esteban, L. Alcázar, M. Torres-Molina, M. Monfort, M. Font-Bardia and A. Escuer, *Inorg. Chem.*, 2012, **51**, 5503; (b) J. Esteban, A. Escuer, M. Font-Bardia, O. Roubeau and S. J. Teat, *Polyhedron*, 2013, **52**, 339; (c) J. Esteban, M. Font-Bardia, J. S. Costa, S. J. Teat and A. Escuer, *Inorg. Chem.*, 2014, **53**, 3194; (d) A. Massard, G. Rogez and P. Braunstein, *Dalton Trans.*, 2014, **43**, 42; (e) A. Escuer, J. Esteban, J. Mayans and M. Font-Bardia, *Eur. J. Inorg. Chem.*, 2014, 5443; (f) M. Pait, A. Bauzá, A. Frontera, E. Colacio and D. Ray, *Inorg. Chem.*, 2015, **54**, 4709; (g) K. I. Alexopoulou, A. Terzis, C. P. Raptopoulou, V. Psycharis, A. Escuer and S. P. Perlepes, *Inorg. Chem.*, 2015, **54**, 5615.

35 (a) F. K. Larsen, J. Overgaard, S. Parsons, E. Rentschler, A. A. Smith, G. A. Timco and R. E. P. Winpenny, *Angew. Chem., Int. Ed.*, 2003, **42**, 5978; (b) M. Rancan, G. N. Newton, C. A. Muryn, R. G. Pritchard, G. A. Timco, L. Cronin and R. E. P. Winpenny, *Chem. Commun.*, 2008, 1560; (c) A. McRobbie, A. R. Sarwar, S. Yeninas, H. Nowell, M. L. Baker, D. Allan, M. Luban, C. A. Muryn, R. G. Pritchard, R. Prozorov, G. A. Timco, F. Tuna, G. F. S. Whitehead and R. E. P. Winpenny, *Chem. Commun.*, 2011, **47**, 6251.

36 (a) E. García-España, P. Gaviña, J. Latorre, C. Soriano and B. Verdejo, *J. Am. Chem. Soc.*, 2004, **126**, 5082; (b) L.-Y. Kong, Z.-H. Zhang, H.-F. Zhu, H. Kawaguchi, T.-A. Okamura, M. Doi, Q. Chu, W.-Y. Sun and N. Ueyama, *Angew. Chem., Int. Ed.*, 2005, **44**, 4352; (c) L. Natrajan, J. Pécaut and M. Mazzanti, *Dalton Trans.*, 2006, 1002; (d) P. C. Andrews, T. Beck, C. M. Forsyth, B. H. Fraser, P. C. Junk, M. Massi and P. W. Roesky, *Dalton Trans.*, 2007, 5651; (e) S.-D. Bian, J.-H. Jia and Q.-M. Wang, *J. Am. Chem. Soc.*, 2009, **131**, 3422; (f) X.-L. Tang, W.-H. Wang, W. Dou, J. Jiang, W.-S. Liu, W.-W. Qin, G.-L. Zhang, H.-R. Zhang, K.-B. Yu and L.-M. Zheng, *Angew. Chem., Int. Ed.*, 2009, **48**, 3499; (g) H. Ke, L. Zhao, G. F. Xu, Y. N. Guo, J. Tang, X. Y. Zhang and H. J. Zhang, *Dalton Trans.*, 2009, 10609; (h) A. M. García-Deibe, C. Portela-García, M. Fondo, A. J. Mota and J. Sanmartín-Matalobos, *Chem. Commun.*, 2012, **48**, 9915; (i) J.-B. Peng, Q.-C. Zhang, X.-J. Kong, Y.-Z. Zheng, Y.-P. Ren, L.-S. Long, R.-B. Huang, L.-S. Zheng and Z. Zheng, *J. Am. Chem. Soc.*, 2012, **134**, 3314; (j) T. D. Pasatoiu, A. Ghirri, A. M. Madalan, M. Affronte and M. Andruh, *Dalton Trans.*, 2014, **43**, 9136.

37 (a) T. N. Hooper, R. Inglis, M. A. Palacios, G. S. Nichol, M. B. Pitak, S. J. Coles, G. Lorusso, M. Evangelisti and E. K. Brechin, *Chem. Commun.*, 2014, **50**, 3498 and references cited therein; (b) A. K. Ghosh, M. Pait, M. Shatruk, V. Bertolasi and D. Ray, *Dalton Trans.*, 2014, **43**, 1970; (c) C. C. Wang, H. Y. Li, X. Q. Zhang, Y. M. Jiang and S. H. Zhang, *J. Cluster Sci.*, 2015, **26**, 1055; (d) V. Velasco, D. Aguilà, L. A. Barrios, I. Borilovic, O. Roubeau, J. Ribas-Ariño, M. Fumanal, S. J. Teat and G. Aromí, *Chem. Sci.*, 2015, **6**, 123; (e) W. Sethi, S. Sanz, K. S. Pedersen, M. A. Sørensen, G. S. Nichol, G. Lorusso, M. Evangelisti, E. K. Brechin and S. Piligkos, *Dalton Trans.*, 2015, **44**, 10315; (f) X.-M. Zhang, P. Li, W. Gao, J.-P. Liu and E.-Q. Gao, *Dalton Trans.*, 2015, **44**, 13581; (g) M. Hołyńska, R. Clérac and M. Rouzières, *Chem. – Eur. J.*, 2015, **21**, 13321.

38 (a) R. D. Shannon, *Acta Crystallogr.*, 1976, **32**, 751; (b) B. Cordero, V. Gómez, A. E. Platero-Prats, M. Revés, J. Echeverría, E. Cremades, F. Barragán and S. Alvarez, *Dalton Trans.*, 2008, 2832.

39 See *e.g.*: (a) P. D. Frischmann and M. J. MacLachlan, *Chem. Soc. Rev.*, 2013, **42**, 871; (b) J.-J. Liu, Y.-F. Guan, Y. Chen, M.-J. Lin, C.-C. Huang and W.-X. Dai, *Dalton Trans.*, 2015, **44**, 9370.

40 H. Lueken, *Magnetochemie*, B.G. Teubner, Stuttgart, 1999.

41 (a) M. Speldrich, H. Schilder, H. Lueken and P. Kögerler, *Isr. J. Chem.*, 2011, **51**, 215; (b) J. van Leusen, M. Speldrich, H. Schilder and P. Kögerler, *Coord. Chem. Rev.*, 2015, **289–290**, 137–148.

42 D. T. Genna, A. G. Wong-Foy, A. J. Matzger and M. S. Sanford, *J. Am. Chem. Soc.*, 2013, **135**, 10586 and references cited therein.

43 W. Keim, *Angew. Chem., Int. Ed. Engl.*, 1990, **29**, 235–244.

44 (a) Y. T. Lai, T. C. Chen, Y. K. Lan, B. S. Chen, J. H. You, C. M. Yang, N. C. Lai, J. H. Wu and C. S. Chen, *ACS Catal.*, 2014, **4**, 3824–3836; (b) H. Guerba, B. Djellouli, C. Petit and V. Pitchon, *C. R. Chim.*, 2014, **17**, 775–784.

45 G. M. Sheldrick, *Acta Crystallogr., Sect. A: Found. Crystallogr.*, 2008, **64**, 112.

This journal is © the Partner Organisations 2016

Inorg. Chem. Front., 2016, **3**, 523–531 | 531